

1 **Understanding Himalayan Erosion and the Significance of the Nicobar Fan**

2

3 Lisa C. McNeill^{*1}, Brandon Dugan², Jan Backman³, Kevin T. Pickering⁴, Hugo F.A. Pouderoux⁵,
4 Timothy J. Henstock¹, Katerina E. Petronotis⁶, Andrew Carter⁷, Farid Chemale, Jr.⁸, Kitty L.
5 Milliken⁹, Steffen Kutterolf¹⁰, Hideki Mukoyoshi¹¹, Wenhuan Chen¹², Sarah Kachovich¹³, Freya L.
6 Mitchison¹⁴, Sylvain Bourlange¹⁵, Tobias A. Colson¹⁶, Marina C.G. Frederik¹⁷, Gilles Guérin¹⁸,
7 Mari Hamahashi^{19**}, Brian M. House²⁰, Andre Hüpers²¹, Tamara N. Jeppson²², Abby R.
8 Kenigsberg²³, Mebae Kuranaga²⁴, Nisha Nair²⁵, Satoko Owari²⁶, Yehua Shan¹², Insun Song²⁷, Marta
9 E. Torres²⁸, Paola Vannucchi²⁹, Peter J. Vrolijk³⁰, Tao Yang^{31***}, Xixi Zhao³², Ellen Thomas³³

10

11 *corresponding author: lcnm@noc.soton.ac.uk

12

13 ¹Ocean and Earth Science, National Oceanography Centre Southampton, University of
14 Southampton, Southampton S014 3ZH, United Kingdom

15 ²Department of Geophysics, Colorado School of Mines, Golden CO 80401, USA

16 ³Department of Geological Sciences, Stockholm University, SE-106 91 Stockholm, Sweden

17 ⁴Earth Sciences, University College London, London WC1E 6BT, United Kingdom

18 ⁵CNRS, UMR6118 - Geosciences Rennes, University de Rennes I, Campus de Beaulieu,
19 35042 Rennes Cedex, France

20 ⁶International Ocean Discovery Program, Texas A&M University, 1000 Discovery Drive, College
21 Station TX 77845, USA

22 ⁷Department of Earth & Planetary Sciences, Birkbeck College, London, WC1E, 7HX, UK

23 ⁸Programa de Pós-Graduação em Geologia, Universidade do Vale do Rio dos Sinos,
24 93.022-000 São Leopoldo - RS Brasil, Brazil

25 ⁹Bureau of Economic Geology, 1 University Station, Box X, Austin TX 78713, USA

26 ¹⁰GEOMAR, Helmholtz Center for Ocean Research Kiel, Wischhofstr. 1-3, Kiel 24148, Germany

27 ¹¹Department of Geoscience, Shimane University, 1060 Nishikawatsu-cho, Matsue, Shimane 690-
28 8504, Japan

29 ¹²Key Laboratory of Marginal Sea Geology, Chinese Academy of Sciences, #511 Kehua Street,
30 Tianhe District, Guangzhou 510640, P.R. China

31 ¹³Department of Geography Planning and Environmental Management, Level 4, Building 35, The
32 University of Queensland, Brisbane, QLD, Australia

33 ¹⁴School of Earth and Ocean Sciences, Cardiff University, Park Place, Cardiff CF10 3XQ, United
34 Kingdom

35 ¹⁵Laboratoire GeoResources, CNRS-Université de Lorraine-CREGU, Ecole Nationale Supérieure
36 de Géologie, Rue du Doyen Marcel Roubault, TSA 70605 – 54518, Vandoeuvre-lès-Nancy, France

37 ¹⁶School of Earth Sciences, University of Western Australia, 35 Stirling Highway, Crawley 6009,
38 Australia

39 ¹⁷Center for Regional Resources Development Technology (PTPSW-TPSA), Agency for the
40 Assessment and Application of Technology (BPPT), Bldg. 820, Earth System Technology
41 (Geotech), Kawasan Puspitek Serpong, South Tangerang, Banten, Indonesia 15314, Indonesia

42 ¹⁸Lamont-Doherty Earth Observatory, Columbia University, Borehole Research Group, 61 Route
43 9W, Palisades NY 10964, USA

44 ¹⁹Geophysics Research Group, Institute of Geology and Geoinformation, Geological Survey of
45 Japan (AIST), AIST Tsukuba Central 7, 1-1-1 Higashi, Tsukuba Ibaraki 305-8567, Japan

46 ²⁰Scripps Institution of Oceanography, University of California, San Diego, Vaughan Hall 434,
47 8675 Discovery Way, La Jolla, CA 92037, USA

48 ²¹MARUM-Center for Marine Environmental Sciences, University of Bremen, PO Box 330 440, D-
49 28334 Bremen, Germany, ahuepers@uni-bremen.de, Tel: (49) 421-21865-814

50 ²²Department of Geology and Geophysics, University of Wisconsin-Madison, 1215 W. Dayton
51 Street, Madison WI 53706, USA

52 ²³Department of Geosciences, Pennsylvania State University, 503 Deike Building, University Park
53 PA 16802, USA

54 ²⁴Graduate School of Science and Engineering, Yamaguchi University, 1677-1 Yoshida
55 Yamaguchi City 753-8512, Japan

56 ²⁵CLCS/Marine Geophysical Division, National Centre for Antarctic and Ocean Research, Earth
57 System Science Organization, Ministry of Earth Sciences, Government of India, Headland Sada,
58 Vasco-da-Gama, Goa – 403804, India

59 ²⁶Department of Earth Sciences, Chiba University, 1-33 Yayoi-cho, Inage-ku, Chiba City 263-8522,
60 Japan

61 ²⁷Geologic Environmental Division, Korea Institute of Geoscience & Mineral (KIGAM), 124
62 Gwahak-ro, Yuseong-gu, Daejeon 34132, Korea

63 ²⁸College of Earth, Ocean and Atmospheric Sciences, Oregon State University, 104 CEOAS Admin
64 Building, Corvallis OR 97331-5503, USA

65 ²⁹Royal Holloway and Bedford New College, Royal Holloway University of London, Queens
66 Building, Egham TW20 0EX, United Kingdom

67 ³⁰New Mexico Tech, 801 Leroy Place, Socorro, NM 87801, USA

68 ³¹Institute of Geophysics, China Earthquake Administration, #5 Minzu Daxue Nanlu, Hiadian
69 District, Beijing 100081, P.R. China

70 ³²Department of Earth and Planetary Sciences, University of California, Santa Cruz, 1156 High
71 Street, Santa Cruz CA 95064, USA

72 ³³Department of Geology and Geophysics, Yale University, New Haven CT 06520-8109, USA

73 **Now at: Earth Observatory of Singapore (EOS), Nanyang Technological University, 50 Nanyang
74 Avenue, Singapore 639798

75 ***Now at: Institute of Geophysics and Geomatics, China University of Geosciences, 388 Lumo
76 Road, Wuhan 430074, PR China

78

79 *Highlights:*

- 80 • Sediment accumulation rates in Nicobar Fan abruptly increase 9.5 Ma
- 81 • Increased sediment flux to eastern Indian Ocean and restructuring of sediment routing
- 82 • Nicobar Fan holds significant record of Indian Ocean sedimentation in late Neogene
- 83 • Shillong Plateau and Indo-Burmese wedge uplift drive sediment south in late Miocene

84

85 *Abstract*

86 A holistic view of the Bengal-Nicobar Fan system requires sampling the full sedimentary section
87 of the Nicobar Fan, which was achieved for the first time by International Ocean Discovery
88 Program (IODP) Expedition 362 west of North Sumatra. We identified a distinct rise in sediment
89 accumulation rate (SAR) beginning ~9.5 Ma and reaching 250-350 m/Myr in the 9.5-2 Ma interval,
90 which equal or far exceed rates on the Bengal Fan at similar latitudes. This marked rise in SAR and
91 a constant Himalayan-derived provenance necessitates a major restructuring of sediment routing in
92 the Bengal-Nicobar submarine fan. This coincides with the inversion of the Eastern Himalayan
93 Shillong Plateau and encroachment of the west-propagating Indo-Burmese wedge, which reduced
94 continental accommodation space and increased sediment supply directly to the fan. Our results
95 challenge a commonly held view that changes in sediment flux seen in the Bengal-Nicobar
96 submarine fan were caused by discrete tectonic or climatic events acting on the Himalayan-Tibetan
97 Plateau. Instead, an interplay of tectonic and climatic processes caused the fan system to develop by
98 punctuated changes rather than gradual progradation.

99

100 *Key Words:* Bengal-Nicobar Fan, submarine fan, Himalayan tectonics, Asian monsoon, Indian
101 Ocean

102

103 *1. Introduction*

104 The Bengal-Nicobar Fan, Indian Ocean (Fig. 1), has the greatest area and length of any
105 submarine fan, and has long been studied to investigate possible links between Himalayan tectonics
106 and the Asian monsoon (e.g., An et al., 2001; Bowles et al., 1978; Clift et al., 2008; Curray, 2014;
107 Curray and Moore, 1974; Curray et al., 1982; France-Lanord et al., 2016; Schwenk and Spiess,
108 2009). To date, a holistic synthesis of the Indian Ocean fan system history and related processes of
109 tectonics, climate and erosion has been hampered by a lack of data from the Nicobar Fan. The
110 importance of sampling widely across a sedimentary system to avoid biases due to major temporal
111 changes in channel and lobe activity was noted (Stow et al., 1990), and highlighted that the under-
112 sampled Nicobar Fan may hold a key component of the eastern Indian Ocean sedimentation record.

113 International Ocean Discovery Program (IODP) Expedition 362 sampled and logged the Nicobar
114 Fan offshore North Sumatra in 2016 (Fig. 1). The stratigraphic results from this expedition (Dugan
115 et al., 2017) are integrated here with results from previous sites on the Bengal-Nicobar Fan and
116 Ninetyeast Ridge (NER) of the Deep Sea Drilling Program (DSDP Leg 22, von der Borch, et al.,
117 1974), Ocean Drilling Program (ODP Leg 116, Cochran et al., 1989; Leg 121, Peirce et al., 1989)
118 and IODP (Expedition 353, Clemens et al., 2016; Expedition 354, France-Lanord et al., 2016). We
119 present the first stratigraphic data from the Nicobar Fan and reappraise published
120 chronostratigraphic data from Bengal Fan and NER drillsites into a unified modern timescale to
121 facilitate accurate comparison of depositional records across the whole system. Comparing
122 sediment accumulation rates (SARs) between these sites gives a new and integrative understanding
123 of the timing of fan growth and distribution of fan deposits.

124

125 *2. Nicobar Fan stratigraphy and sediment source*

126 Expedition 362 drilled two sites on the northern Nicobar Fan east of the NER (Fig. 1), sampling
127 the complete sedimentary section at Site U1480 to a basement depth of 1415 meters below seafloor
128 (mbsf), and from 1150 mbsf to within 10's m of basement at Site U1481 at 1500 mbsf. At both sites

129 Units I and II represent the Nicobar Fan, with Units III-V representing intervals dominated by
130 pelagic sedimentation with significantly reduced SARs (Fig. 1).

131 Bengal Fan sediments are predominantly micaceous quartzo-feldspathic sands of the Ganges and
132 Brahmaputra that drain the Himalaya and southern Tibet plus contributions from the Meghna river
133 that drains northeastern India and Bangladesh (France-Lanord et al., 2016). Despite proximity to the
134 Sunda forearc, the Nicobar Fan sediments at Sites U1480 and U1481 (Fig. S1) contain a similar
135 range of siliciclastic sediment gravity-flow (SGF) deposits (mostly turbidites) as Bengal Fan sites.
136 The sand- and silt-size grain assemblage in the Nicobar Fan is relatively uniform downhole as
137 quartzo-feldspathic (arkosic) sands, with pelitic metamorphic lithic grains, mica, minor detrital
138 carbonate (<5%), minor woody debris, and an abundant and diverse assemblage of mostly high-
139 grade metamorphic heavy minerals (including kyanite and sillimanite). Candidate sources for the
140 Nicobar Fan include the Himalayan-derived Ganges-Brahmaputra, Indo-Burman Ranges/West
141 Burma, Sunda forearc and arc, and NER. Detrital zircon age spectra of samples from the Nicobar
142 Fan sand-silt SGF deposits are dominantly sourced from the Greater and Tethyan Himalaya mixed
143 with sediment from the Burmese arc-derived Paleogene Indo-Burman Ranges, similar to the
144 provenance of Neogene sands deposited in the eastern Bengal and Surma basins (Najman et al.,
145 2008, 2012) (Figs. 1-3). The limited arc-derived ash content in sediments at Sites U1480-1481
146 suggests that the Sunda forearc makes only a minor contribution. Significant input from the
147 Irrawaddy drainage is unlikely as it would require transfer of material across the forearc and
148 possibly the trench. Cenozoic sediment isopachs of the Martaban back arc basin, the main north–
149 south-oriented depocentre in the Andaman Sea related to the development of the Thanlwin-
150 Irrawaddy delta system, show no obvious evidence for major routing to the west where carbonate-
151 capped volcanic highs (e.g. Yadana High) served as a barrier for most of the Neogene (Racey and
152 Ridd, 2015). Nevertheless we consider Irrawaddy sources in our provenance interpretations.

153

154 3. Bengal-Nicobar Fan Sediment Accumulation Patterns

155 Age-depth distributions of calcareous nannofossils, planktonic foraminifers, diatoms,
156 silicoflagellates, and radiolarians were used to create tie points for SARs for Expedition 362 sites
157 (Dugan et al., 2017) (Fig. 4A; Supplementary Material). Also, published latest Eocene-Recent
158 biomagnetostratigraphic data from six representative DSDP, ODP and IODP Bengal Fan and NER
159 sites were reassessed and placed on a common time scale (Hilgen et al., 2012; Pälike et al., 2006)
160 (Fig. 4; Supplementary Material). The reassessment of previous biostratigraphic data and the choice
161 of age model tie points considered recent developments in understanding the consistency and
162 reliability of biohorizons in lower latitude environments. At all sites, the age-depth relationship is
163 non-linear. At Sites U1480 and U1481 on the Nicobar Fan, the SAR increases dramatically at 9.5-9
164 Ma, from <15 m/Myr to >200 m/Myr, which corresponds to the onset of significant fan deposition
165 at the Unit III-II boundary. Specifically, at Site U1480 rates increase from 2-15 to 223 m/Myr, and
166 at Site U1481 from 11-27 to 207 m/Myr (Figs. 4, S2). At Site U1480, high rates persist and in the
167 earliest Pleistocene (~2-2.5 Ma), they increase further to 360 m/Myr (Fig. S2). In the Bengal Fan,
168 such high rates, of the order of 250-300 m/Myr or greater, are only found within the more proximal
169 fan (e.g., Weber et al., 1997, although greater spatial and temporal variability in rates might be
170 expected here due to high impact of sea level fluctuation coupled with shifting channel/levée
171 systems) or in the latest Pleistocene (e.g., Expedition 354 results of France-Lanord et al., 2016).
172 These results emphasize the significance of the Nicobar Fan within the wider Bengal-Nicobar Fan
173 system from the late Miocene to early Pleistocene (~9-2 Ma).

174 The NER (separating the Bengal and Nicobar fans) is thought to capture an elevated expression
175 of fan deposition despite its predominantly pelagic composition (Peirce et al., 1989), due to
176 increased flow lofting (cf., Stow et al., 1990) and nepheloid layer flux. Remarkably, at all northern
177 NER sites (216, 217 and 758/1443; Fig. 2B) SARs increase by a factor of 2-3 at ~10-8 Ma, coeval
178 with the Nicobar Fan site increases. Decreasing carbonate content values at Sites 217, 758, 1443,
179 support that the increase in SAR resulted from the effect of increased input of clay.

180 When SARs increase on the Nicobar Fan and NER (at 2-9°N), rates on the Bengal Fan at related
181 mid-fan positions (Fig. 4A) show either a marked decrease (e.g., Site 718, at 1°S) or minimal
182 change (e.g., Site 1451, at 8°N), and all rates are lower than on the Nicobar Fan immediately after
183 9-9.5 Ma. At Site 718, rates decrease from 275 to 12-13 m/Myr at 9.5 Ma and only exceed 100
184 m/Myr in the late Pleistocene (Fig. S2). At Site 1451, rates from 9.5 Ma do not exceed 150 m/Myr
185 (range: 70-150 m/Myr; Fig. S4). Local variations in deposition between Leg 116 sites (717, 718,
186 719) can be explained by late Miocene folding on the Indian plate controlling accommodation and
187 potential submarine-channel routing (Stow et al., 1990).

188 Depositional history at a single site is inevitably affected by individual channel and lobe
189 positions and there will be variability across the fan in terms of sediment accumulation due to
190 depositional environment, e.g., channel-axis, channel-margin, levee-overbank, lobe and lobe fringe
191 etc. (e.g., Stow et al., 1990; Schwenk and Spiess, 2009). However, on the Nicobar Fan seismic
192 horizons and packages can be traced over large distances with confidence in unit correlation and
193 with minimal evidence of unit thickness variation across and along the oceanic plate. No onlap in
194 the vicinity of the drillsites is observed, and channel-levée complexes that might correlate with
195 enhanced deposition are evenly distributed spatially and temporally (Dugan et al., 2017). In
196 addition, our analysis of data from other Expedition 354 Bengal Fan transect sites where SARs may
197 be greater than at Site U1451 (e.g., U1450, France-Lanord et al., 2016) continues to support that
198 during the late Miocene and Pliocene, Nicobar Fan rates either exceeded or were broadly
199 comparable with those on the Bengal Fan. This interpretation is further supported because the
200 Expedition 354 sites on the Bengal Fan are located 5°N of the Expedition 362 sites on the Nicobar
201 Fan (and therefore probably in a more proximal position).

202 Preliminary benthic foraminiferal data from the Site U1480 pre-fan and lowermost Nicobar Fan
203 deposits indicate that this part of the Indian plate was at upper abyssal depths (2500-3000 m;
204 Supplementary Material), not isolated at a higher elevation which could delay arrival of fan
205 sediments. Combining these facts, we have confidence that the drillsite stratigraphic record is

206 representative of the wider Nicobar Fan.

207 Compilation of age-depth plots and SARs from across the fan system enables us to examine
208 earlier sedimentation patterns. These indicate that by at least 15 Ma, SARs on the Bengal Fan were
209 high with sediment directed west of the NER (Fig. 5C). The oldest recovered sediments in the
210 central part of the Bengal Fan are Oligocene (25-28 Ma) thin-bedded silts, and the first significant
211 sands are late Miocene, although this may be related to changes in coring technique and recovery
212 (9-10 Ma: Site U1451, France-Lanord et al., 2016). At other Expedition 354 sites, the apparent
213 earliest onset of substantial sand was <8 Ma (Sites U1450 and U1455), although we note that low
214 recovery in parts of the deeper section at these sites may allow for the presence of additional earlier
215 thick sand layers. In the distal Bengal Fan (Leg 116 Sites 717–719), early Miocene (back to 17 Ma)
216 silts came from the Himalaya and minor components from the Indian subcontinent (Cochran et al.,
217 1989; Bouquillon et al., 1990; Copeland et al., 1990). At Nicobar Fan Site U1481, a 20-m interval
218 within the period 19-9 Ma (sample 362-9 in Figs. 2&3) includes minor very fine-grained sandstones
219 and siltstones, with the same zircon assemblage as other Expedition 362 sand/silt samples (Fig. 2),
220 supporting an eastern Himalayan source. These predate the dramatic increase in sediment flux to the
221 Nicobar Fan sites.

222 In summary, although the Bengal-Nicobar Fan was clearly developing prior to the late Miocene,
223 the SARs at a range of sites support a marked increase in sediment flux at around 9.5 Ma, in
224 particular to the eastern part of the system, the Nicobar Fan (Fig. 5B; an idea postulated by Bowels
225 et al. (1978), confirmed here with detailed and integrated drilling and seismic data). A major
226 conclusion from our appraisal of SARs is that when high SARs are recorded on the Bengal Fan,
227 they are significantly lower on the Nicobar Fan, and that between ~9.5–2 Ma this switches abruptly
228 (Fig. 3), with highest sediment flux deflected to the east.

229

230 *4. Nicobar Fan volumetrics and late Miocene-Recent growth of the Sunda forearc*

231 Using sediment thickness from seismic profiles and ocean drilling boreholes, we have made a

232 new estimate of the late Miocene-Recent Nicobar Fan volume, incorporating the component of fan
233 now accreted into the Sunda subduction margin (see Supplementary Material). Estimates of the
234 present day Nicobar Fan volume are $\sim 0.5 \times 10^6 \text{ km}^3$ (Figs. 1, S4; Supplementary Material), without
235 decompaction. An additional $0.4 \times 10^6 \text{ km}^3$ is estimated to have been added to the accretionary prism
236 between the Nicobar Islands and Southern Sumatra, using present day sediment thicknesses and
237 plate convergence rates back to 9 Ma (Fig. S5). This generates a minimum late Miocene-Recent (i.e.
238 from ~ 9.5 Ma to present) Nicobar Fan volume of $\sim 1 \times 10^6 \text{ km}^3$. This volume is significant compared
239 with the estimated Bengal Fan volume of $7.2 \times 10^6 \text{ km}^3$ for the entire Neogene, a period of ~ 20 Myr
240 (Clift, 2002).

241 The increase in thickness of the Indian plate sediment section at ~ 9.5 Ma would have
242 corresponded to a marked and abrupt change in sediment volume input to the north Sunda margin.
243 Offshore North Sumatra and the Nicobar Islands, the forearc prism is markedly wide (150-180 km)
244 and thick relative to the rest of the margin and to other accretionary prisms (McNeill and Henstock,
245 2014), and the northern Sumatran prism forms an unusual plateau inferred to be a consequence of
246 internal and basal material properties and/or prism growth history (e.g., Fisher et al., 2007). The
247 large additional sediment input volume from 9.5 Ma to present in the easternmost Indian Ocean is a
248 significant proportion of the prism volume and can explain the anomalously large northern Sunda
249 prism (supporting hypotheses by Hamilton, 1973; Karig et al., 1979).

250

251 5. Discussion

252 Our new integrated Nicobar-Bengal Fan sediment records show a net increase in flux to the
253 eastern Indian Ocean at 9.5-9 Ma, representing the onset of a new sedimentary regime in the east
254 Indian Ocean. Detrital zircon ages (Fig. 2) and petrology from the Nicobar Fan sediments show the
255 sand provenance remained unchanged throughout the middle Miocene to present. To constrain
256 sources we compared these results with detrital zircon ages from potential source regions in the
257 Himalayas as well as the Burmese arc and Irrawady drainage due to the presence of Cenozoic age

258 zircons (mainly between 60-20 Ma). Comparison of the zircon age distributions (Fig. 3) show SGF
259 deposits exposed on the Andaman-Nicobar Islands are closely similar to Nicobar Fan sediments and
260 that both have affinities with Himalayan-derived units, the Trans-Himalaya and arc-derived input
261 from erosion of the Indo-Burman Ranges that were expanding westwards during the Pliocene.
262 These are the same sources as Neogene sands deposited in the northeast Bengal and Surma basins
263 via the paleo-Brahmaputra River (Najman et al., 2012) (Fig. 1). Between 15-9 Ma the northeast
264 Bengal Basin underwent inversion related to tectonic shortening and exhumation of the Shillong
265 Basin Plateau which accommodates up to 1/3 of the present-day convergence across the Eastern
266 Himalaya (Bilham and England, 2001; Biswas et al., 2007; Clark and Bilham, 2008) (Fig. 1).
267 Exhumation and erosion of the Himalayan-derived Surma Group atop the Shillong Plateau began at
268 this time followed by the main phase of surface uplift < 3.5 Ma (Najman et al., 2016) - these
269 timings provide an excellent fit with the high SARs on the Nicobar Fan (from 9.5, and 2.5-2 Ma).
270 We propose that this inversion of the Shillong region and westward migration of the Indo-Burmese
271 wedge reduced accommodation and diverted sediments south to the shelf and Nicobar Fan. The
272 most significant sediment pulse to the Nicobar Fan, at 2.5-2 Ma, may also record erosion of the
273 exhumed eastern Himalayan syntaxis and resulting erosion, with at least 12 km of material since 3
274 Ma - a signal recorded in the Surma Basin from the latest Pliocene (Bracciali et al., 2016) but not
275 previously identified in the Indian Ocean. From ~ 2 Ma, a SAR reduction on the Nicobar Fan
276 supports the hypothesis that impingement of the NER on the Sunda Trench diverted the primary
277 flux west of the ridge with concomitant high mid-late Pleistocene SARs on the Bengal Fan (e.g.,
278 France-Lanord et al., 2016) (Fig. 5A), although westward re-routing of the Brahmaputra River may
279 also have played a role (Najman et al., 2016).

280 The Nicobar Fan is volumetrically significant within the Bengal-Nicobar Fan system, and at
281 certain times during the late Miocene-early Pleistocene, such as the near 400 m/Myr SARs of the
282 earliest Pleistocene, it may have been a dominant sediment sink. Since 10 Ma, sea level has
283 generally fallen (Miller et al., 2005), decreasing accommodation on the shelf, thus amplifying the

284 processes driving sediment southward to the fan. Erosion was probably aided by South Asian
285 monsoon strengthening in the mid to late Miocene (e.g., An et al., 2001; Betzler et al., 2016; Kroon
286 et al., 1991; Peterson and Backman, 1990; Prell and Kutzbach, 1992) combined with the orographic
287 forcing that caused the locus of monsoon precipitation to shift south onto the newly uplifted
288 Shillong Plateau (Biswas et al., 2007). Enhanced erosion rates (Duvall et al., 2012) and/or uplift in
289 the eastern Tibetan plateau (e.g., An et al., 2001) in the late Miocene would also contribute to the
290 volume of sediment available.

291 Avulsion of large-scale channel-levée complexes is common to many submarine fans
292 (e.g., Amazon Fan; Flood et al., 1991). We propose that the eastward deflection of sediment
293 towards the Nicobar Fan at 9.5 Ma was the result of channel avulsion in response to increased
294 sediment flux. Consequently, the proportion of sediment routed from the northeastern Bengal Basin
295 to the Bengal Fan was significantly reduced. Any differential seafloor topography on the shelf and
296 the subsiding NER could have assisted this eastward diversion process. Similar processes have been
297 observed in physical flume experiments, for example, lobe switching observed with change in
298 sedimentation supply/rate, accommodation, and depositional slope (Fernandez et al., 2014; Parsons
299 et al., 2002).

300 An early, lower-volume phase of fan deposition is recorded in the accreted sediments of the
301 Sunda forearc (to ~40-50 Ma; Curray and Moore, 1974; Curray et al., 1979; Karig et al., 1980). A
302 model of trench-axial supply, with sediment now almost entirely accreted, can explain this earlier
303 phase (nascent Nicobar Fan), with trench overspill delivering minor sands/silts recorded at Site
304 U1481 by the middle Miocene.

305 An accurate history of siliciclastic deposition on the Bengal-Nicobar Fan system necessitates
306 knowledge of both fans. Using estimates of fan volume, we demonstrate that the Nicobar Fan is
307 significant within the overall sediment budget of the Bengal-Nicobar Fan, particularly from 9.5-2
308 Ma. An interplay of tectonic, climatic and sedimentological processes, rather than a discrete
309 tectonic or climatic event or mechanism such as monsoon onset, as often invoked (e.g., Betzler et

310 al., 2016; Clift et al., 2008), moved sediment through a series of staging areas and controlled SARs
311 in the various sediment sinks of the Indo-Asian system. Our reappraisal of integrated drilled fan
312 data is inconsistent with the long-held notion of gradual fan progradation (Curry et al., 2003) but
313 rather suggests a more dynamic system of punctuated and abrupt changes (Fig. 5D). Our work
314 highlights the importance of sediment routing from the uplifting Eastern Himalaya along the eastern
315 Indian Ocean to the Nicobar Fan during the late Neogene, a region whose role has been
316 significantly underappreciated.

317

318 *Acknowledgements*

319 This research used samples and data provided by the International Ocean Discovery Program
320 (IODP) (www.iodp.org/access-data-and-samples). The JOIDES Resolution crew and IODP
321 technical team are thanked for their contributions during Expedition 362. We thank the editor and
322 two reviewers for their valuable comments which helped to improve the paper. McNeill
323 acknowledges support during and following the Expedition from Natural Environment Research
324 Council grant NE/P012817/1.

325

326 *References*

- 327 Allen, R., Najman, Y., Carter, A., Barfod, D., Bickle, M.J., Chapman, H.J., Garzanti, E., Vezzoli,
328 G., Andò, S., Parrish, R. 2008. Provenance of the Tertiary sedimentary rocks of the Indo-Burman
329 Ranges, Burma (Myanmar): Burman arc or Himalayan-derived? *J. Geol. Soc. London* 165 (6),
330 1045–1057.
- 331 An, Z., Kutzbach, J.E., Prell, W.L., Porter, S.C. 2001. Evolution of Asian monsoons and phased
332 uplift of the Himalaya-Tibetan plateau since Late Miocene times. *Nature* 411, 62–66.
333 doi:10.1038/35075035.

334 Bandopadhyay, P.C., Ghosh, B. 2015. Provenance analysis of the Oligocene turbidites (Andaman
 335 Flysch), South Andaman Island: A geochemical approach. *J. Earth Syst. Sci.* 124, 1019–1037.
 336 doi:10.1007/s12040-015-0586-5.

337 Betzler, C., and 29 others, 2016. The abrupt onset of the modern South Asian Monsoon winds.
 338 *Scientific Reports* 6, 29838. doi:10.1038/srep29838.

339 Bilham, R., England, P. 2001. Plateau "pop-up" in the great 1897 Assam earthquake. *Nature* 410,
 340 806–809. doi:10.1038/35071057

341 Biswas, S., Coutand, I., Grujic, D., Hager, C., Stockli, D., Grasemann, B. 2007. Exhumation and
 342 uplift of the Shillong plateau and its influence on the eastern Himalayas: new constraints from
 343 apatite and zircon (U-Th-[Sm])/He and apatite fission track analyses. *Tectonics* 26, TC6013.
 344 doi:10.1029/2007TC002125.

345 Bouquillon, A., France-Lanord, C., Michard, A., Tiercelin, J.-J. 1990. Sedimentology and isotopic
 346 chemistry of the Bengal Fan sediments: The denudation of the Himalaya, in: Cochran, J.R., Stow,
 347 D.A.V. et al., Leg 116 Distal Bengal Fan. *Proc. ODP Sci. Res.* 116, College Station, TX, Ocean
 348 Drilling Program. doi:10.2973/odp.proc.sr.116.1990

349 Bowles, F.A., Ruddiman, W.F., Jahn, W.H. 1978. Acoustic stratigraphy, structure, and depositional
 350 history of the Nicobar Fan, eastern Indian Ocean. *Mar. Geol.* 26, 269–288.
 351 [http://dx.doi.org/10.1016/0025-3227\(78\)90063-4](http://dx.doi.org/10.1016/0025-3227(78)90063-4).

352 Bracciali, L., Najman, Y., Parrish, R.R., Akhter, S.H., Millar, I. 2015. The Brahmaputra tale of
 353 tectonics and erosion: Early Miocene river capture in the Eastern Himalaya. *Earth Planet. Sci. Lett.*
 354 415, 25–37.

355 Bracciali, L., Parrish, R., Najman, Y., Smye, A., Carter, A., Wijbrans, J.R. 2016. Plio-Pleistocene
 356 exhumation of the eastern Himalayan syntaxis and its domal "pop-up". *Earth-Science Rev.* 160,
 357 350–385. <http://dx.doi.org/10.1016/j.earscirev.2016.07.010>.

358 Campbell, I.H., Reiners, P.W., Allen, C.M., Nicolescu, S., Upadhyay, R., 2005. He–Pb double
 359 dating of detrital zircons from the Ganges and Indus Rivers: Implication for quantifying

360 sediment recycling and provenance studies, *Earth Planet. Sci. Lett.* 237, 402–432.
361 <http://dx.doi.org/10.1016/j.epsl.2005.06.043>.

362 Clark, M., Bilham, R. 2008. Miocene rise of the Shillong Plateau and the beginning of the end for
363 the Eastern Himalaya. *Earth Planet. Sci. Lett.* 269, 337–351.
364 <http://dx.doi.org/10.1016/j.epsl.2008.01.045>.

365 Clemens, S.C., Kuhnt, W., LeVay, L.J. et al. 2016. *Indian Monsoon Rainfall*. Proc. IODP 353,
366 College Station, TX, International Ocean Discovery Program.
367 <http://dx.doi.org/10.14379/iodp.proc.353.2016>.

368 Clift, P. 2002. A brief history of the Indus River, in: Clift, P., Kroon, D., Gaedicke, C., Craig, J.
369 (Eds.), *Tectonic and climatic evolution of the Arabian Sea region*, Geol. Soc. London, Spec.
370 Publ. 195, 97–116.

371 Clift, P.D., Hodges, K.V., Heslop, D., Hannigan, R., van Long, H., Calves, G. 2008. Correlation of
372 Himalayan exhumation rates and Asian monsoon intensity, *Nat. Geosci.* 1, 875–880.
373 doi:10.1038/ngeo351.

374 Cochran, J.R., Stow, D.A.V. et al., 1989. Leg 116 Distal Bengal Fan. Proc. ODP Init. Repts. 116,
375 College Station, TX, Ocean Drilling Program. doi:10.2973/odp.proc.ir.116.1989.

376 Cochran, J.R., Stow, D.A.V. et al., 1990. Leg 116 Distal Bengal Fan. Proc. ODP Sci. Res. 116,
377 College Station, TX, Ocean Drilling Program. doi:10.2973/odp.proc.sr.116.1990.

378 Curray, J.R. 2014. The Bengal depositional system: From rift to orogeny. *Mar. Geol.* 352, 59–69.
379 <http://dx.doi.org/10.1016/j.margeo.2014.02.001>.

380 Curray, J.R., Moore, D.G. 1974. Sedimentary and tectonic processes in the Bengal deep-sea fan and
381 geosyncline, in: Burk, C.A., Drake, C.L. (Eds.), *Continental margins*, New York, Springer,
382 617–627.

383 Curray, J.R., Moore, D.G., Lawver, L.A., Emmel, F.J., Raitt, R.W., Henry, M., Kiekheffer, R. 1979.
384 *Tectonics of the Andaman Sea and Burma*, in: Watkins, J., Montadert, L., Dickerson, P.W.
385 (Eds.), *Tectonics of the Andaman Sea and Burma*, Am. Ass. Petr. Geol., Mem. 29, 189–198.

Curray, J.R., Emmel, F.J., Moore, D.G. 2003. The Bengal Fan: morphology, geometry, stratigraphy,
history and processes. *Mar. Petrol. Geol.* 19, 1191–1223. [http://dx.doi.org/10.1016/S0264-8172\(03\)00035-7](http://dx.doi.org/10.1016/S0264-8172(03)00035-7).

Dugan, B., McNeill, L.C., Petronotis, K.E., and the Expedition 362 Scientists. 2017. Expedition 362
Preliminary Report: Sumatra Subduction Zone. Intern. Ocean Discovery Program.
[doi:10.14379/iodp.pr.362.2017](https://doi.org/10.14379/iodp.pr.362.2017)

Duvall, A.R., Clark, M.K., Avdeev, B., Farley, K.A., Chen, Z. 2012. Widespread late Cenozoic
increase in erosion rates across the interior of eastern Tibet constrained by detrital low-
temperature thermochronometry. *Tectonics* 31, TC3014. [doi:10.1029/2011TC002969](https://doi.org/10.1029/2011TC002969).

Fernandez, R.L., Cantelli, A., Pirmez, C., Sequeiros, O., and Parker, G., 2014. Growth patterns of
subaqueous depositional channel lobe systems developed over a basement with a downdip break
in slope: Laboratory experiments, *Journal of Sedimentary Research*, 84, 168–182.
[doi:10.2110/jsr.2014.10](https://doi.org/10.2110/jsr.2014.10)

Flood, R.D., Manley, P.C., Kowsman, R.O., Appi, C.J., Pirmez, C. 1991. Seismic facies and late
Quaternary growth of Amazon Submarine Fan, in: Weimer, P., Link, M.H. (Eds.), *Seismic facies
and sedimentary processes of submarine fans and turbidite systems*, New York, Springer-Verlag,
415–433.

France-Lanord, C., Spiess, V., Klaus, A., Schwenk, T. et al. 2016. Bengal Fan. *Proc. IODP 354*,
College Station, TX, International Ocean Discovery Program.
<http://dx.doi.org/10.14379/iodp.proc.354.2016>.

Fisher, D., Mosher, D., Austin, J.A., Gulick, S.P., Masterlark, T., Moran, K. 2007. Active
deformation across the Sumatran forearc over the December 2004 Mw 9.2 rupture. *Geology* 35,
99–102. [doi:10.1130/G22993A.1](https://doi.org/10.1130/G22993A.1).

Gehrels, G., Kapp, P., DeCelles, P., Pullen, A., Blakey, R., Weislogel, A., Ding, L., Guynn, J.,
Martin, A., McQuarrie, N., Yin, A. 2011. Detrital zircon geochronology of pre-Tertiary strata in
the Tibetan-Himalayan orogen. *Tectonics* 30, 1944–1994. [doi:10.1029/2011TC002868](https://doi.org/10.1029/2011TC002868).

412 Hall, R. 2012. Late Jurassic-Cenozoic reconstructions of the Indonesian region and the Indian
 413 Ocean. *Tectonophys.* 570–571, 1–41. <http://dx.doi.org/10.1016/j.tecto.2012.04.021>.
 414 Hamilton, W. 1973. Tectonics of the Indonesia region. *Geol. Soc. Malaysia Bull.* 6, 3–10.
 415 Hilgen, F.J., Lourens, L.J., and Van Dam, J.A., 2012. The Neogene Period, in: Gradstein, F.M.,
 416 Ogg, J.G., Schmitz, M.D., Ogg, G.M. (Eds.), *The Geological Time Scale 2012*, Amsterdam,
 417 Elsevier, 2, 923–978.
 418 Karig, D.E., Suparka, S., Moore, G.F., Hehanussa, P.E. 1979. Structure and Cenozoic evolution of
 419 the Sunda arc in the Central Sumatra region, in: Watkins, J., Montadert, L., Dickerson, P. (Eds.),
 420 Geological and Geophysical Investigations of Continental Slopes and Rises, Amer. Assoc. Petrol.
 421 Geol. Mem. 29, 223–237.
 422 Karig, D.E., Lawrence, M.B., Moore, G.E., Curray, J.R. 1980. Structural framework of the forearc
 423 basin, NW Sumatra. *J. Geol. Soc. London* 137, 77–91.
 424 Kroon, D., Steens, T., Troelstra, S.T. 1991. Onset of monsoonal related upwelling in the western
 425 Arabian sea as revealed by planktonic foraminifers. *Proc. ODP Sci. Res.* 117, College Station,
 426 TX, Ocean Drilling Program, 257–263. doi:10.2973/odp.proc.sr.117.126.1991.
 427 Limonta, M., Resentini, A., Carter, A., Bandopadhyay, P.C., Garzanti, E. 2017. Provenance of
 428 Oligocene Andaman sandstones (Andaman–Nicobar Islands): Ganga–Brahmaputra or Irrawaddy
 429 derived? in: Bandopadhyay, P.C., Carter, A. (Eds.), *The Andaman–Nicobar Accretionary Ridge:*
 430 *Geology, Tectonics and Hazards.* *Geol. Soc. London Mem.* 47, 143–154.
 431 McNeill, L.C., Henstock, T.J. 2014. Forearc structure and morphology along the Sumatra-Andaman
 432 subduction zone. *Tectonics* 33, 112–134. doi:10.1002/2012TC003264.
 433 Miller, K.G., Kominz, M.A., Browning, J.V., Wright, J.D., Mountain, G.S., Katz, M.E., Sugarman,
 434 P.J., Cramer, B.S., Christie-Blick, N., Pekar, S.F. 2005. The Phanerozoic record of global sea-
 435 level change. *Science* 310, 1293–1298. doi:10.1126/science.1116412.

436 Moore, D.G., Curray, J.R., Raiti, R.W., Emmel, F.J. 1974. Stratigraphic-seismic section correlations
 437 and implications to Bengal Fan history. *Init. Repts. DSDP* 22, U.S. Govt. Print. Off., 403–412.
 438 doi:10.2973/dsdp.proc.22.116.1974.

439 Najman, Y., Bickle, M., Boudagher-Fadel, M., Carter, A., Garzanti, E., Paul, M., Wijbrans, J.,
 440 Willett, E., Oliver, G., Parrish, R., Akhter, H., Allen, R., Ando, S., Christy, E., Reisberg, L.,
 441 Vezzoli, G. 2008. The Paleogene record of Himalayan erosion, Bengal Basin, Bangladesh. *Earth*
 442 *Planet. Sci. Lett.* 273, 1–14. <http://dx.doi.org/10.1016/j.epsl.2008.04.028>.

443 Najman, Y., Allen, R., Willett, E.A.F., Carter, A., Barfod, D., Garzanti, E., Wijbrans, J., Bickle,
 444 M.J., Vezzoli, G., Ando, A., Oliver, G., Uddin, M.J. 2012. The record of Himalayan erosion
 445 preserved in the sedimentary rocks of the Hatia Trough of the Bengal Basin and the Chittagong
 446 Hill Tracts, Bangladesh. *Basin Research* 24, 1–21. doi:10.1111/j.1365-2117.2011.00540.x.

447 Najman, Y., Bracciali, L., Parrish, R.R., Chisty, E., Copley, A. 2016. Evolving strain partitioning in
 448 the Eastern Himalaya: The growth of the Shillong Plateau. *Earth Planet. Sci. Lett.* 433, 1–9.
 449 <http://dx.doi.org/10.1016/j.epsl.2015.10.017>.

450 Parsons, J.D., Schweller, W.J., Stelting, C.W., Southard, J.B., Lyons, W.J., Grotzinger, J.P. 2002. A
 451 preliminary experimental study of turbidite fan deposits. *J. Sed. Res.* 72, 619–628.
 452 doi:10.1306/032102720619.

453 Peirce, J., Weissel, J. et al. 1989. *Proc. ODP Init. Repts.*, 121, College Station TX, Ocean Drilling
 454 Program. doi:10.2973/odp.proc.ir.121.1989.

455 Peterson, L.C., and Backman, J., 1990. Late Cenozoic carbonate accumulation and the history of
 456 the carbonate compensation depth in the western equatorial Indian Ocean. *Proc. ODP Sci. Res.*
 457 115, College Station, TX, Ocean Drilling Program, 467–508.
 458 doi:10.2973/odp.proc.sr.115.163.1990.

459 Pälike, H., Norris, R.D., Herrle, J.O., Wilson, P.A., Coxall, H.K., Lear, C.H., Shackleton, N.J.,
 460 Tripathi, A.K., Wade, B.S. 2006. The heartbeat of the Oligocene climate system, *Science* 314,
 461 1894–898. doi:10.1126/science.1133822.

462 Prell, W.L., Kutzbach, J.E. 1992. Sensitivity of the Indian monsoon to forcing parameters and
 463 implications for its evolution *Nature* 360, 647–652. doi:10.1038/360647a0.

464 Racey, A. & Ridd, M. F. 2015. Petroleum Geology of Myanmar. *Geol. Soc. London, Memoirs*, 45,
 465 63–81.

466 Schwenk, T., and Spiess, V. 2009. Architecture and stratigraphy of the Bengal Fan as response to
 467 tectonic and climate revealed from high-resolution seismic data, *SEPM Spec. Pub.*, 92, 107-131.

468 Stow, D.A.V., Amano, K., Balson, P.S., Brass, G.W., Corrigan, J., Raman, C.V., Tiercelin, J.-J.,
 469 Townsend, M., Wijayananda, N.P. 1990. Sediment facies and processes on the distal Bengal Fan,
 470 Leg 116. *Proc. ODP Sci. Res.* 116, College Station, TX, Ocean Drilling Program, 377–396.
 471 doi:10.2973/odp.proc.sr.116.110.1990.

472 von der Borch, C.C., Sclater, J.G. et al., 1974. *Init. Repts. DSDP 22*, Washington, U.S. Govern.
 473 Print. Office. doi:10.2973/dsdp.proc.22.1974.

474

475 *Figure Captions*

476 Figure 1. Regional map of study area. Map includes Bengal-Nicobar Fan system, river systems,
 477 eastern Himalayan provinces, and relevant DSDP/ODP/IODP sites. BB= Bengal Basin;
 478 SP=Shillong Plateau; SB=Surma Basin; IBR=Indo-Burman Ranges. Inset summarizes Site U1480
 479 lithostratigraphy.

480

481 Figure 2. Detrital zircon age plots for samples and equivalent plots of regional rivers and formations.
 482 TH= Tethyan Himalaya; GHS=Greater Himalaya Series; LHS=Lesser Himalaya Series. Details of
 483 Expedition 362 samples are given in Table S1.

484

485 Figure 3. Detrital zircon age comparison plots of samples from this study and regional rivers and
 486 formations. Multidimensional scaling maps (Vermeesch, 2013) based on calculated K–S distances
 487 between U–Pb age spectra, comparing Nicobar Fan sand samples from this study with possible

488 source areas compiled from the literature (Allen et al., 2008; Bracciali et al., 2015; 2016; Campbell
489 et al., 2005; Gehrels et al., 2011; Limonta et al., 2017; Najman et al., 2008). The maps show 362
490 samples share the same sources as the SGF deposits exposed on the Andaman-Nicobar Islands and
491 Neogene sediments deposited in northeast Bengal that were originally sourced from erosion of the
492 Indo-Burma Ranges. The IODP sands are not directly comparable to sands from the modern
493 Brahmaputra or Irrawaddy. See Figure 2 for acronyms.

494

495 Figure 4. Age-depth relationships at ocean drilling sites. Panel (A) shows tie points of
496 biomagnetostratigraphic age-depth relationships for Bengal Fan sites (718C, U1451) and Nicobar
497 Fan sites (U1480, U1481). Panel (B) shows biomagnetostratigraphic tie points of age-depth
498 relationships for sites from the Ninetyeast Ridge crest (216, 217, 758A, 1443A). Inset shows
499 sediment accumulation rate (SAR) increase between 9 and 10 Ma. Data are presented in detail in
500 Figures S2 and S3, and Tables S2 and S3.

501

502 Figure 5. Conceptual model of Bengal-Nicobar Fan system history (tectonics from Hall (2012); fan
503 morphology from Bowles et al. (1978) and Curray (2014); fan data from DSDP/ODP/IODP sites
504 (white dots; red dots=Expedition 362 sites). A) Late Pleistocene to Recent, sedimentation primarily
505 on Bengal Fan, B) late Miocene-Pliocene, Nicobar Fan dominates, C) pre-late Miocene, Bengal Fan
506 dominates, minor trench-axial supply to Sunda margin/Nicobar Fan. D) Pattern of sedimentation
507 along the Bengal Fan system from proximal (left) to distal (right) indicating absence of simple fan
508 progradational pattern (updated from Curray et al., 2003). Data sources: Indo-Burman Ranges and
509 Andaman-Nicobar forearc data (Bandopadhyay and Ghosh, 2015; Curray et al., 2003 and references
510 therein); ocean drilling site data (Cochran et al., 1989, 1990; France-Lanord et al., 2016; von der
511 Borch et al., 1974; this study). All sites converted to modern timescale (Supplementary Material).
512 Note that 9.5-18 Ma silts for Nicobar Fan sites are only present at Site U1481.

513

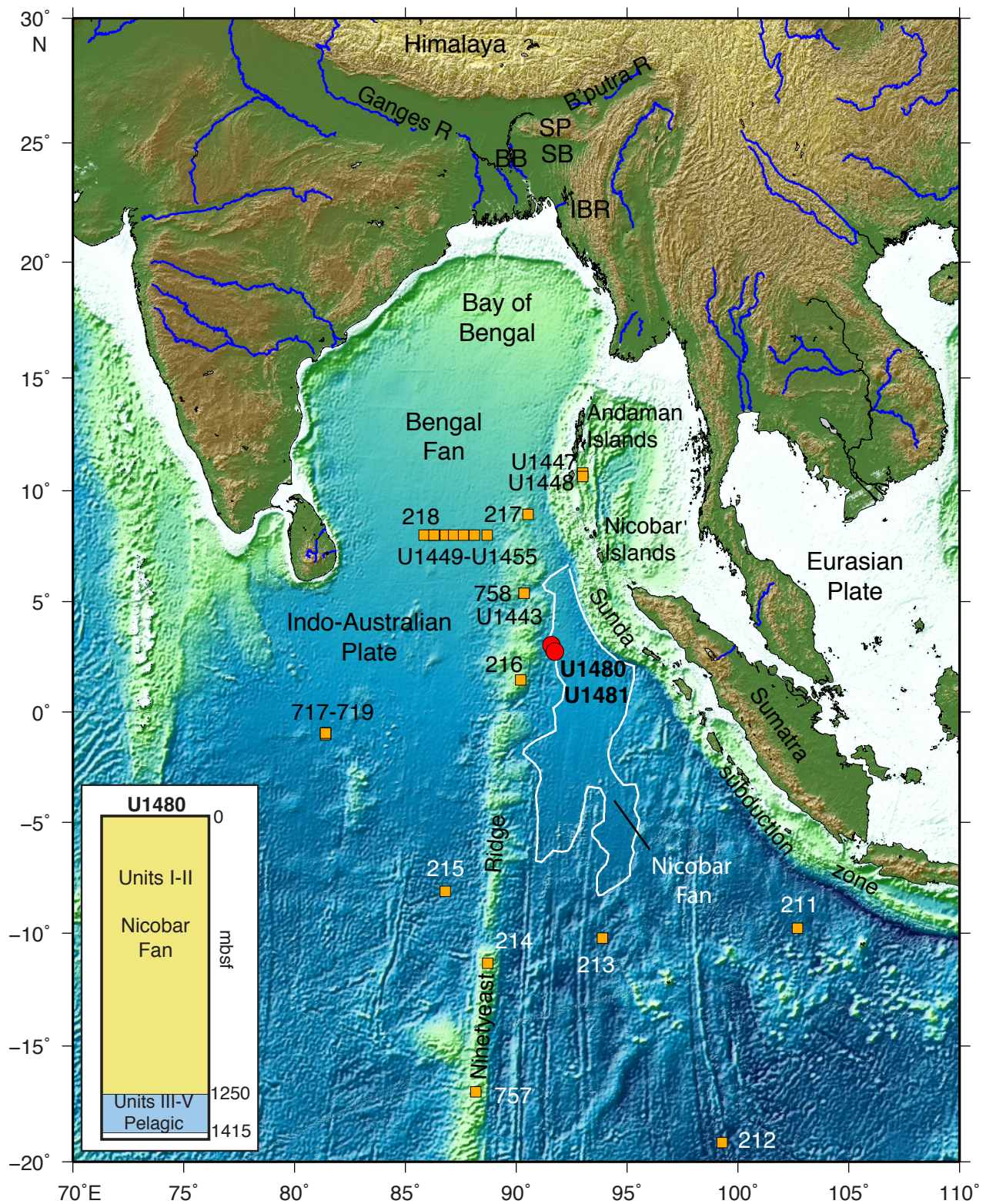
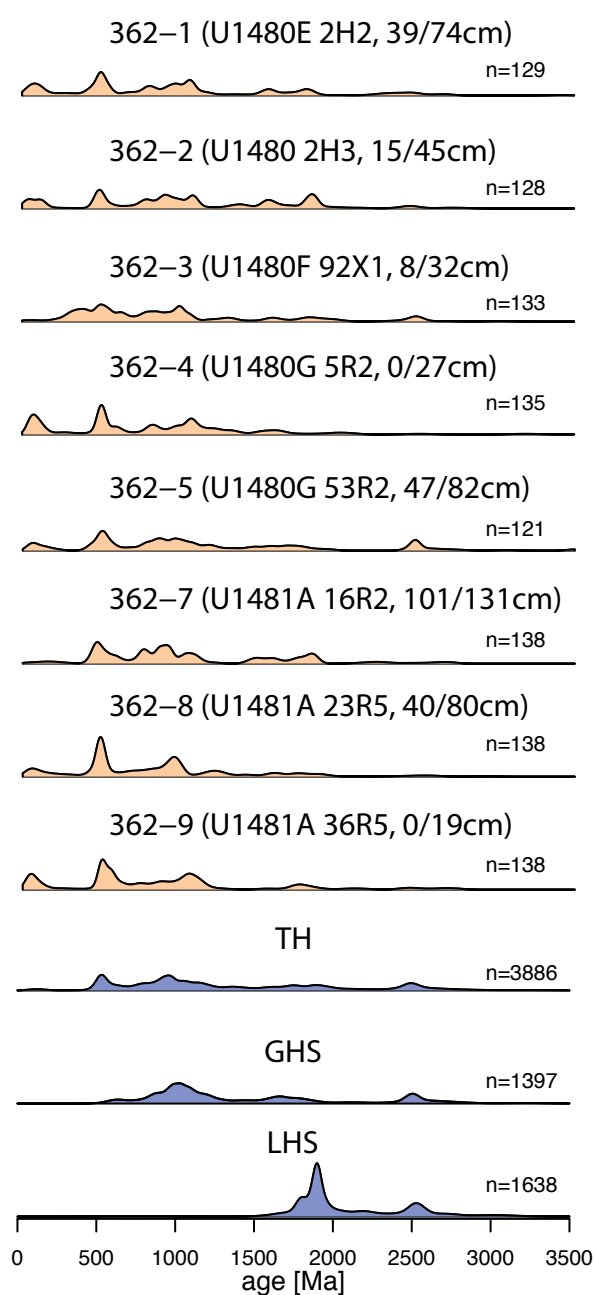
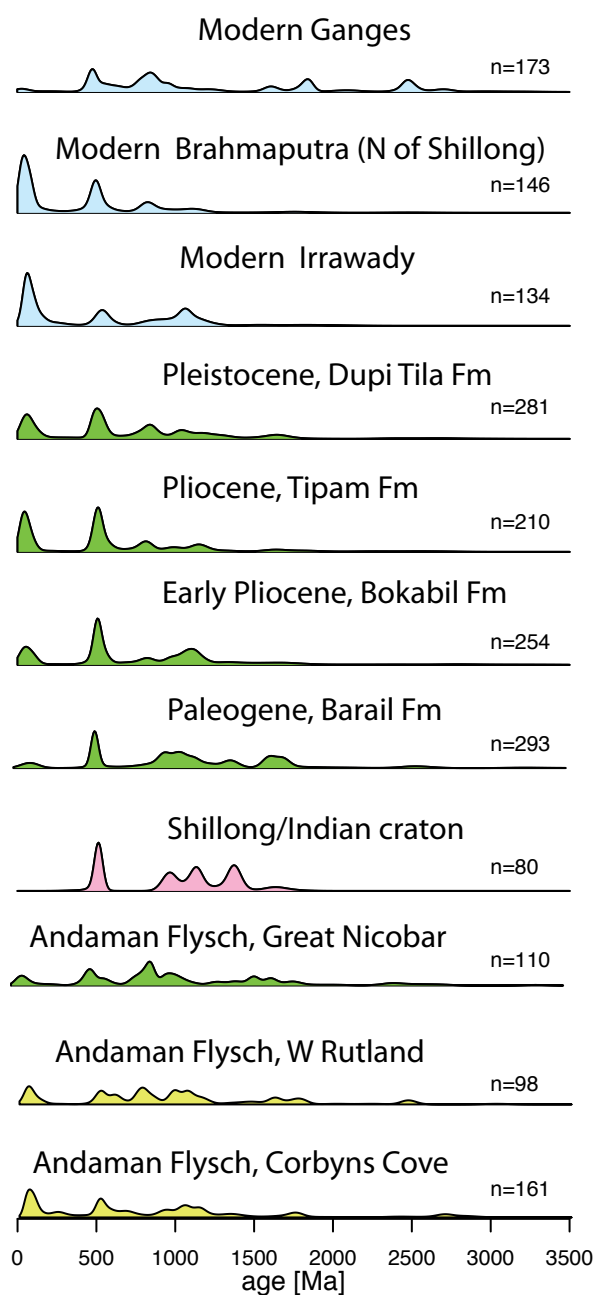
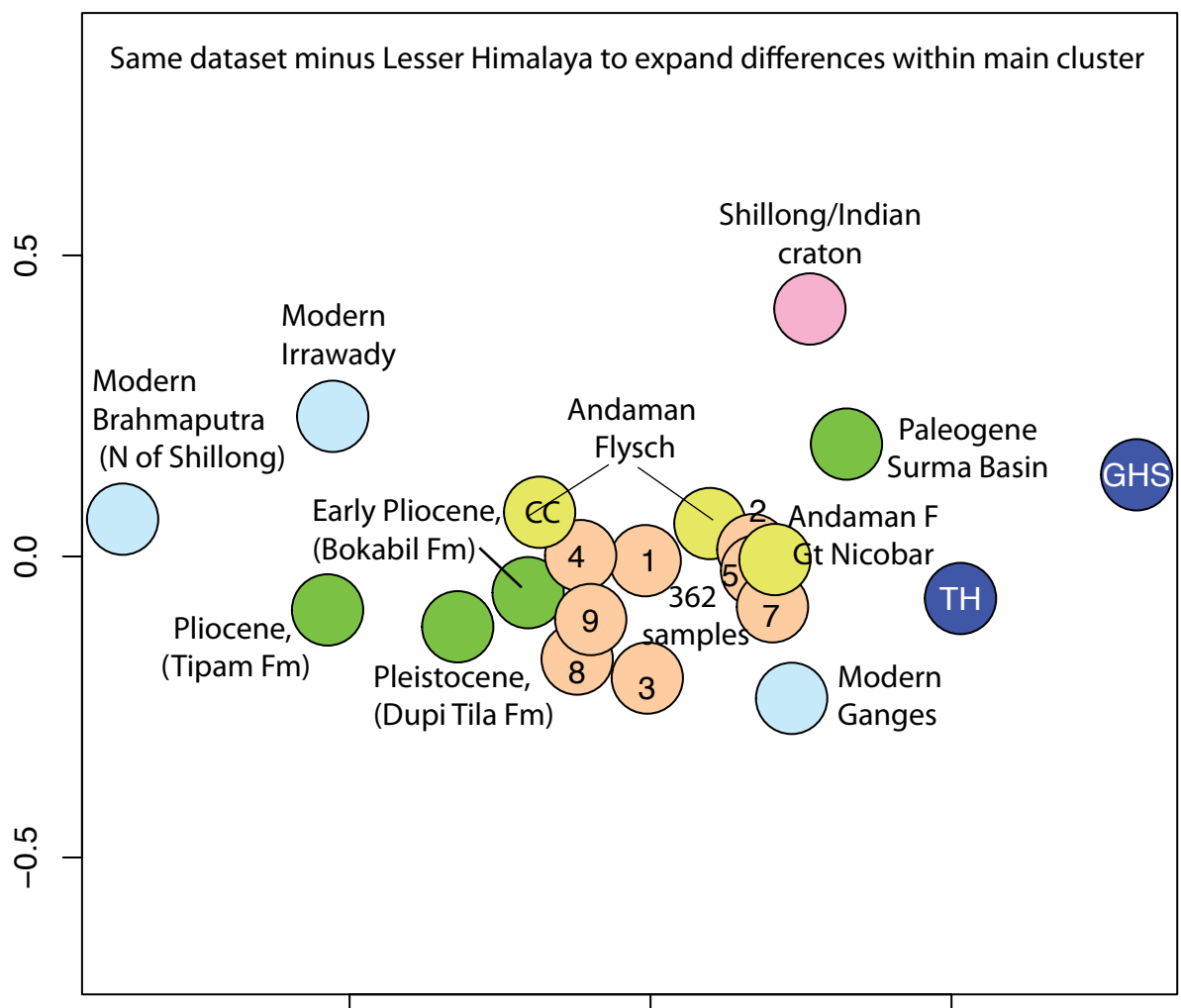
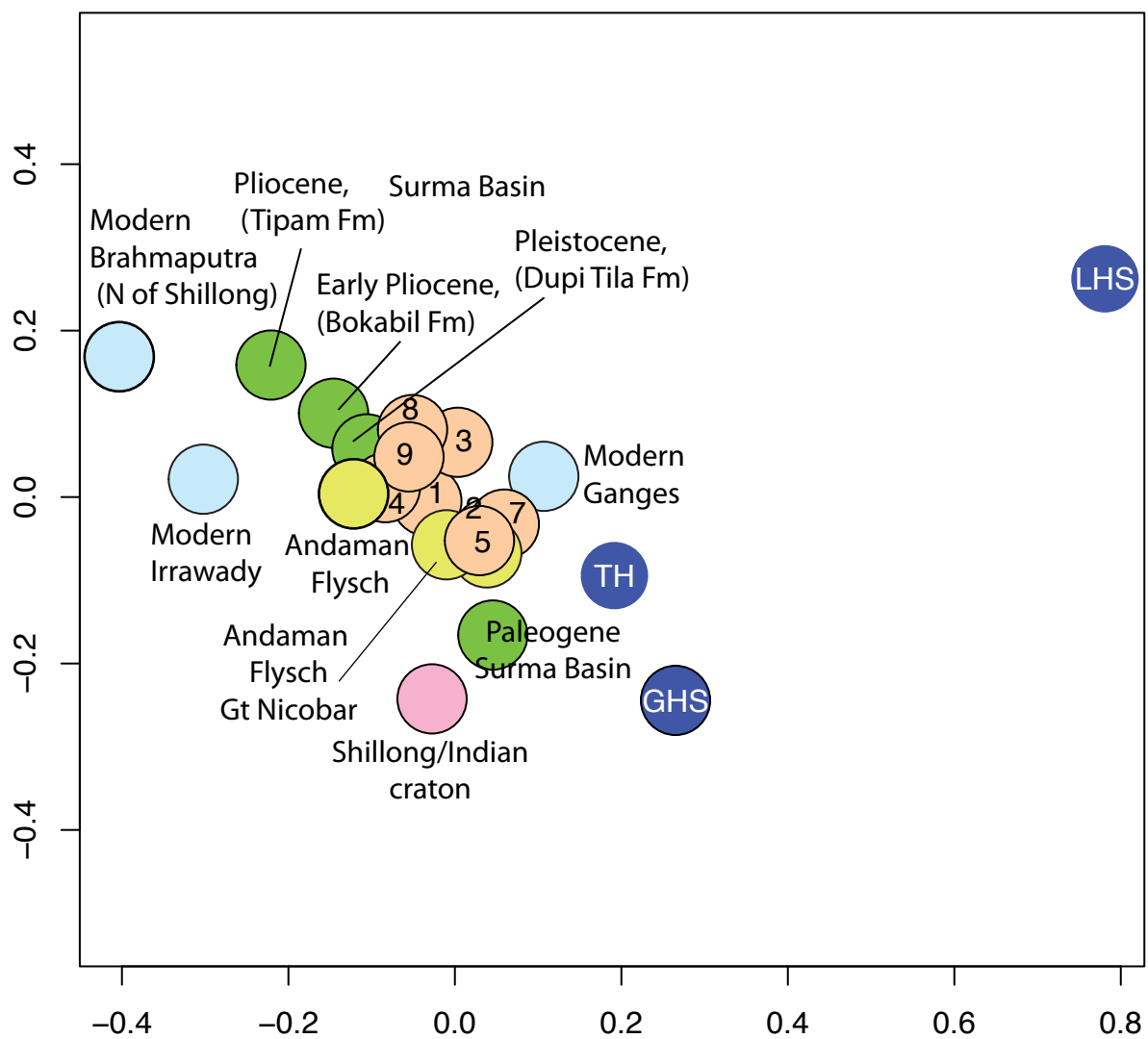


Figure 1.





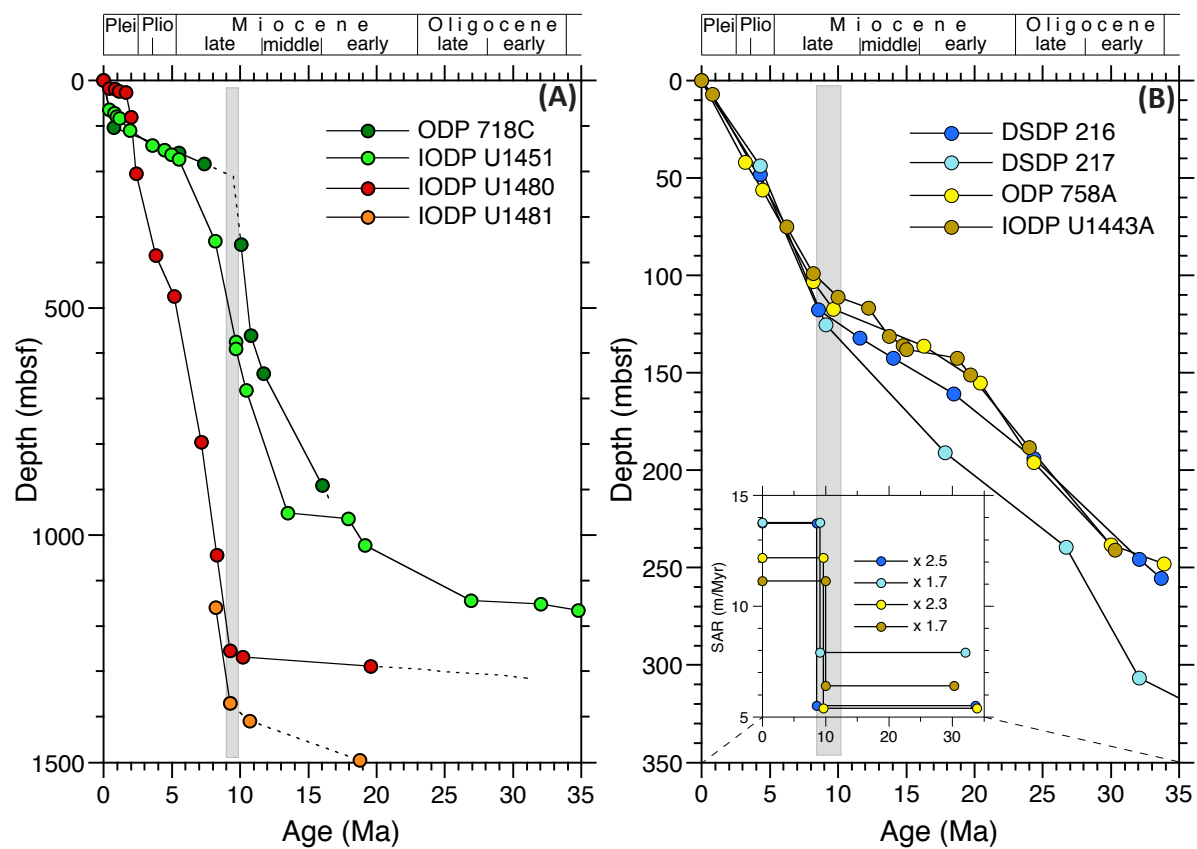


Figure 4.

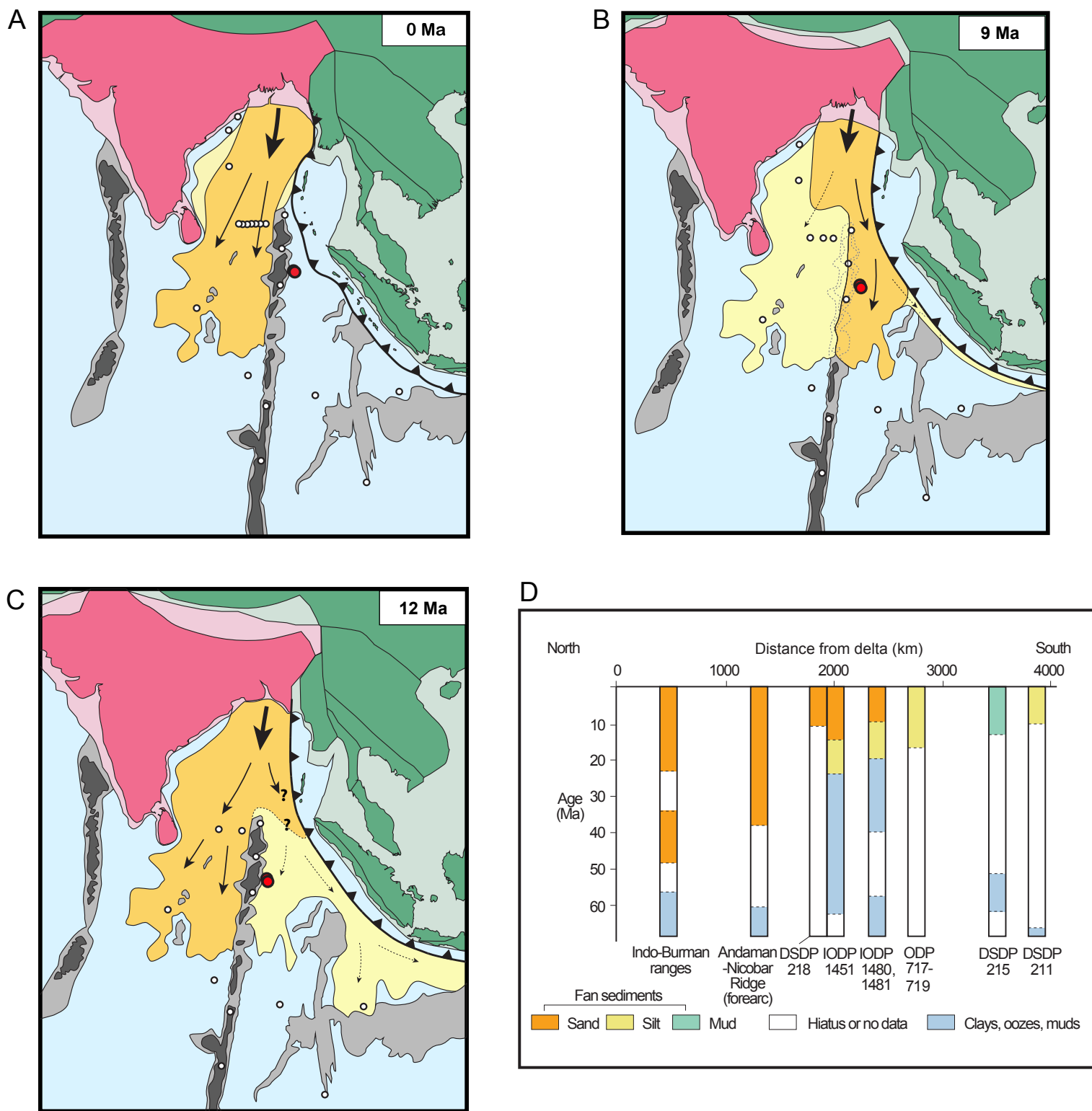


Figure 5.